Molecular Therapy
Nucleic Acids
Original Article

A cell-penetrating peptide enhances delivery and efficacy of phosphorodiamidate morpholino oligomers in *mdx* mice

Li Gan,[1] Leslie C.L. Wu,[1] Jenna A. Wood,[1] Monica Yao,[1] Chris M. Treleaven,[1] Nelsa L. Estrella,[1] Bruce M. Wentworth,[1] Gunnar J. Hanson,[1] and Marco A. Passini[1]

[1]Sarepta Therapeutics, Inc., 215 First Street Cambridge, Cambridge, MA 02142, USA

Antisense RNA technology is a strategy for the treatment of Duchenne muscular dystrophy (DMD), a progressive and universally fatal X-linked neuromuscular disease caused by frameshift mutations in the gene encoding dystrophin. Phosphorodiamidate morpholino oligomers (PMOs) are an antisense RNA platform that is used clinically in patients with DMD to facilitate exon skipping and production of an internally truncated, yet functional, dystrophin protein. Peptide-conjugated PMOs (PPMOs) are a next-generation platform in which a cell-penetrating peptide is conjugated to the PMO backbone, with the goal of increasing cellular uptake. RC-1001 is a PPMO that contains a proprietary cell-penetrating peptide and targets the *Dmd* mutation in *mdx* mice. It was evaluated in *mdx* mice for exon 23 skipping, dystrophin production, and functional efficacy. Single-dose RC-1001 dose dependently increased exon skipping and dystrophin protein levels in striated muscle and is associated with improvements in muscle function. Dystrophin protein levels were durable for 60 days. Three doses, each given 1 month apart, increased exon skipping to 99% in quadriceps and 43% in heart, with dystrophin protein levels at 39% and 9% of wild type, respectively. These findings support clinical development of PPMO therapies for the treatment of DMD.

INTRODUCTION

Duchenne muscular dystrophy (DMD) is a rare, progressive, fatal, degenerative neuromuscular disease with X-linked recessive inheritance caused by mutations in the *DMD* gene, encoding dystrophin.[1,2] These mutations disrupt the messenger RNA (mRNA) reading frame and result in production of little or no dystrophin, a crucial component of the protein complex that connects the cytoskeleton of a muscle fiber to the extracellular matrix.[1,3–5] In the absence of dystrophin, the mechanical stress of muscle contraction causes membrane instability and muscle damage.[6] The progression of DMD involves irreversible decline, beginning with reduced muscle strength, difficulty walking, and developmental delays, followed by loss of ambulation and, ultimately, death from respiratory or cardiac failure.[2,4]

One current therapeutic strategy for DMD is the use of rationally designed antisense oligonucleotides (ASOs) that target specific sequences within the pre-mRNA transcript and modulate alternative splicing or block aberrant, disease-causing splice sites.[7] Directed exon skipping with ASOs enables restoration of the *DMD* mRNA reading frame.[8–11] This results in the translation of an internally truncated, yet functional, dystrophin protein. The theory of exon skipping emanated from what is known as the reading-frame rule: out-of-frame deletions or duplications lead to the absence of dystrophin and a more severe DMD phenotype, whereas in-frame mutations that lead to the production of shortened, functional proteins are associated with the milder DMD phenotype.[5,12] Among various chemically modified ASOs, phosphorodiamidate morpholino oligomers (PMOs) showed a widespread increase of dystrophin production with a favorable safety profile in murine and canine models of DMD.[13–18] To date, there are four US Food and Drug Administration (FDA)-approved PMO therapies for patients with DMD: eteplirsen (Exondys 51)[19] for patients amenable to exon 51 skipping, golodirsen (Vyondys 53)[20] and viltolarsen (Viltepso)[21] for patients amenable to exon 53 skipping, and casimersen (Amondys 45)[22] for patients amenable to exon 45 skipping. Accelerated FDA approval was granted to these PMOs based on the surrogate endpoint of increased dystrophin production in skeletal muscle that is likely to predict clinical benefit in patients with DMD. Longer-term studies of eteplirsen and golodirsen (2–3 years) have suggested that these agents preserve ambulatory and pulmonary function in patients with amenable *DMD* mutations.[23–27] Although these therapies represent a major advance in the treatment of DMD, delivery to target tissues and cellular uptake could be improved.[28] Pre-clinical data especially suggest that drug delivery to cardiomyocytes is limited.[17,28] Moreover, current PMO therapies require weekly dosing to achieve and sustain clinical benefit in DMD.[15,18–21,25,29,30] While the introduction of home-based infusions has alleviated the burden of treatment in terms of travel, weekly treatments still require a considerable commitment of time and effort,

Received 1 March 2022; accepted 14 August 2022;
https://doi.org/10.1016/j.omtn.2022.08.019.

Correspondence: Jenna A. Wood, Sarepta Therapeutics, Inc. 215 First Street Cambridge, MA 02142, USA.
E-mail: medicalpublications@sarepta.com

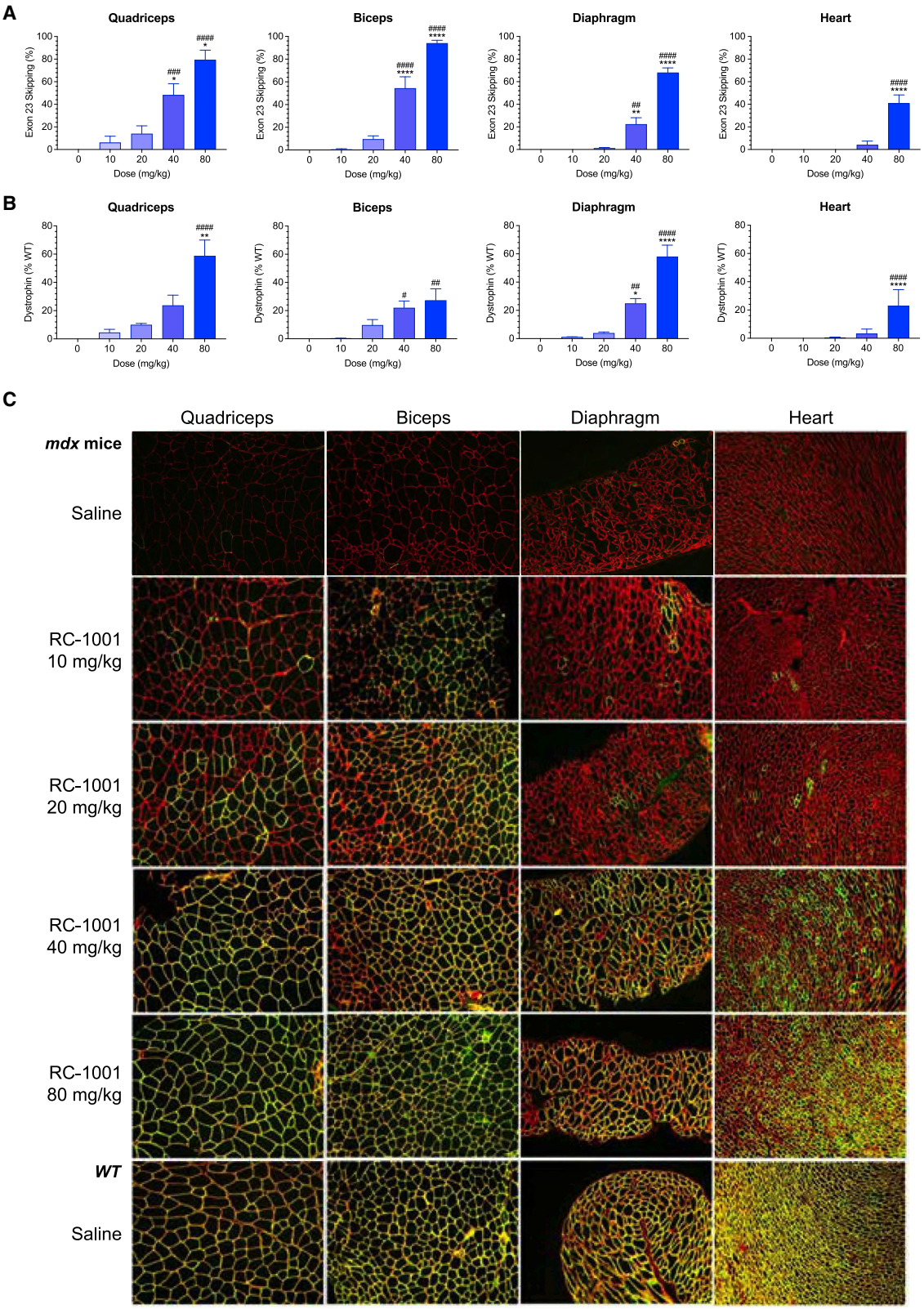

(legend on next page)

indicating that reduction in dosing frequency would be a desirable attribute.[31]

Peptide-conjugated PMOs (PPMOs) are a next-generation chemistry platform in which a cell-penetrating peptide is conjugated to the PMO backbone, with the goal of increasing cellular uptake, exon skipping, and dystrophin levels.[32] Pre-clinical work has shown that in certain instances, PPMOs can be dosed less frequently than corresponding PMOs to produce dystrophin, reduce disease pathology, and increase skeletal and cardiac muscle function.[33–38]

In the current study, we conjugated a proprietary cell-penetrating peptide to a *Dmd* exon 23-skipping PMO and tested the delivery of the resulting PMO compound, RC-1001, *in vivo*.[39] We examined exon skipping, dystrophin levels, and muscle function 30 days after a single systemic dose in the *mdx* mouse model of DMD. The durability of exon skipping and dystrophin production was also evaluated after a single RC-1001 dose. Finally, pharmacodynamic effects of repeated monthly dosing with RC-1001 or its PMO counterpart AVI-4225 were examined throughout 13 weeks.

RESULTS

PPMO dose response and functional recovery in *mdx* mice

A single intravenous injection of RC-1001 targeting mouse dystrophin exon 23 was administered to *mdx* mice, and biological and functional outcomes were assessed over 30 days. RC-1001 treatment resulted in dose-dependent increases in exon skipping on day 30 at doses >20 mg/kg in skeletal muscle (Figure 1A; Table S1). Averages of 9.5%, 54.4%, and 94.0% exon skipping were observed in biceps muscle from mice injected with RC-1001 20, 40, and 80 mg/kg, respectively, with significant ($p < 0.0001$) increases in exon skipping at the 40 and 80 mg/kg doses versus saline controls. In diaphragm muscle, observed exon skipping was 1.1%, 22.4%, and 68.0% ($p < 0.005$ versus saline controls for 40 and 80 mg/kg doses). RC-1001 treatment also resulted in exon skipping in the heart at the 40 and 80 mg/kg doses with averages of 4.2% and 40.9%, respectively. Exon skipping in the heart was significantly higher than saline controls for the 80 mg/kg dose ($p < 0.0001$).

Consistently, RC-1001 treatment resulted in dose-dependent increases in protein level at dosages >20 mg/kg in skeletal muscle (Figures 1B and S1; Table S1). Averages of 9.7%, 22.0%, and 27.3% of wild-type dystrophin levels were observed in biceps muscle and 3.9%, 24.9%, and 58.0% were observed in diaphragm muscle from mice injected with RC-1001 20, 40, and 80 mg/kg, respectively, with significant increases at the 40 and 80 mg/kg doses compared with saline controls ($p < 0.05$). In the heart, an increase in dystrophin protein levels of 3.3% and 23.1% of wild type was observed after treatment with RC-1001 40 and 80 mg/kg, respectively, with significant increases in dystrophin protein levels at the 80 mg/kg dose compared with saline controls ($p < 0.0001$).

Immunohistochemical analysis showed low to moderate levels of dystrophin-positive cells with RC-1001 10 and 20 mg/kg in the quadriceps and biceps (Figure 1C). A dose-dependent increase in dystrophin-positive myofibers in striated muscle was observed, with near wild-type expression levels in skeletal muscle myofibers at 80 mg/kg.

Functional testing was performed weekly after RC-1001 injection (Figure 2A). Measurable improvements in grip strength were evident with the lowest RC-1001 dose of 10 mg/kg. Significant improvements in grip strength were observed at 20 mg/kg ($p < 0.001$) and reached wild-type levels at 40 ($p < 0.0001$) and 80 mg/kg ($p < 0.0001$; Figure 2B). Increased strength was not due to a change in bodyweight, as treatment with RC-1001 did not have an effect on the weight of *mdx* mice (data not shown).

Measurable improvements in motor coordination on the rotarod test were also observed in mice administered RC-1001 20 mg/kg, with peak performances at 40 and 80 mg/kg ($p < 0.0001$). Functional recovery in RC-1001-treated *mdx* mice with RC-1001 20 mg/kg corresponded to exon skipping levels of approximately 10%–15% and dystrophin protein levels of 10% in skeletal muscle (Table S1).

Single-dose PPMO in *mdx* mice: Durability of dystrophin protein production

To examine the durability of PPMO treatment, a single systemic dose of RC-1001 40 mg/kg was administered to *mdx* mice, and tissues were examined at 7, 30, 60, and 90 days post injection (Figure 3A). RC-1001 resulted in significant increases in exon 23 skipping in the quadriceps, diaphragm, and heart of *mdx* mice by day 7 (all $p < 0.0001$ versus saline controls) (Figure 3B). Exon 23 skipping steadily declined over time in all three muscles examined but continued to be detectable in quadriceps, diaphragm, and heart at 90, 60, and 30 days after dosing, respectively. At the protein level, an average of 20.7%, 14.5%, and 2.0% of wild-type dystrophin expression was observed in quadriceps, diaphragm, and heart, respectively, at day 7 (Figure 3C). Dystrophin protein levels declined more slowly than exon skipping and were still detectable in all three muscle groups at day 90 (Figure 3D). These

Figure 1. RC-1001 dose response in *mdx* mice

(A and B) Exon skipping (RT-PCR) (A) and dystrophin protein level (western blot) (B) in quadriceps, biceps, diaphragm, and heart were analyzed 30 days after a single dose of RC-1001. Each bar represents mean ± SEM (n = 6). (C) Representative immunohistochemistry images of skeletal muscle and heart from *mdx* mice treated with saline or with RC-1001 at 10, 20, 40, and 80 mg/kg and wild-type controls. A dose-dependent increase in dystrophin-positive cells (green) in quadriceps, biceps, diaphragm, and heart was observed, which co-localized with laminin (red) on the basal lamina. One-way ANOVA was conducted to understand whether the means were different among groups, and Tukey multiple comparison test was performed to understand the difference between the groups. *$p < 0.05$, **$p < 0.005$, ***$p < 0.0005$, or ****$p < 0.0001$ versus the previous dose group. #$p < 0.05$, ##$p < 0.005$, ###$p < 0.0005$, or ####$p < 0.0001$ versus the saline-treated group. ANOVA, analysis of variance; SEM, standard error of mean, WT, wild type.

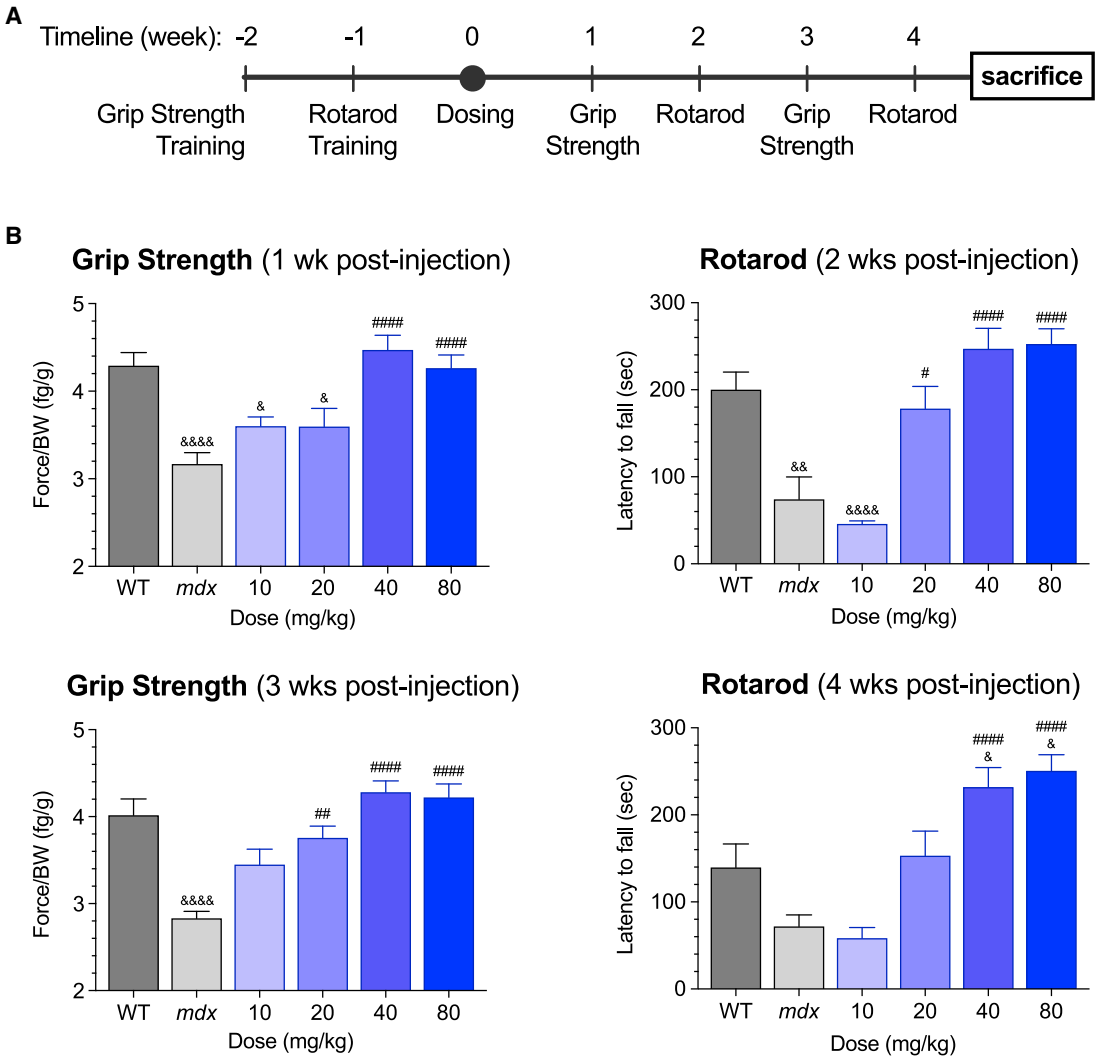

Figure 2. Functional assessment of RC-1001 dose response

(A) Timeline for dosing and functional measurements. (B) Mice were tested for grip strength at 7 and 21 days post dose and for rotarod at 14 and 28 days post dose. Each bar represents mean ± SEM. One-way ANOVA was conducted to understand whether the means were different among groups, and Tukey multiple comparison test was performed to understand the difference between the groups. #p < 0.05, ##p < 0.005, ###p < 0.0005, or ####p < 0.0001 versus the saline-treated group. &p < 0.05, &&p < 0.005, &&&p < 0.0005, or p < 0.0001 versus WT mice. ANOVA, analysis of variance; SEM, standard error of mean; WT, wild type.

observations indicate a prolonged pharmacologic effect of a single RC-1001 dose. Immunofluorescence staining of the quadriceps showed dystrophin-positive myofibers in RC-1001-treated *mdx* mice at all four time points examined, with proper localization of the internally truncated dystrophin protein to the sarcolemma (Figure 3E). Moreover, dystrophin protein was widespread throughout the myofibers in the quadriceps in *mdx* mice at all time points examined.

Repeated dosing of PPMO and PMO in *mdx* mice

Repeated dosing experiments were undertaken to determine whether exon skipping and dystrophin protein levels could be increased and to compare the effects of the RC-1001 PPMO with its PMO (not peptide-conjugated) counterpart AVI-4225. Both compounds were administered at 40 mg/kg once monthly and evaluated at day 35 (5 weeks after a single dose), day 63 (5 weeks after the second dose) or day 91 (5 weeks after the third dose) (Figure 4A). Compared with a single dose, three doses of RC-1001 40 mg/kg increased exon skipping from 82.6% to 98.8% in the quadriceps, from 49.1% to 87.4% in the diaphragm, and from 13.4% to 43.2% in the heart (Figure 4B). Correspondingly, the RC-1001–generated dystrophin protein levels increased from 19.8% to 38.9%, from 26.4% to 50.9%, and from 3.3% to 8.6% of wild type (Figures 4C and 4D). In comparison, *mdx* mice treated with AVI-4225 had significantly lower exon 23 skipping (day 91; 53.4% in the quadriceps, 0.5% in the diaphragm, and 0% in the heart; all p < 0.0001 versus RC-1001) and dystrophin

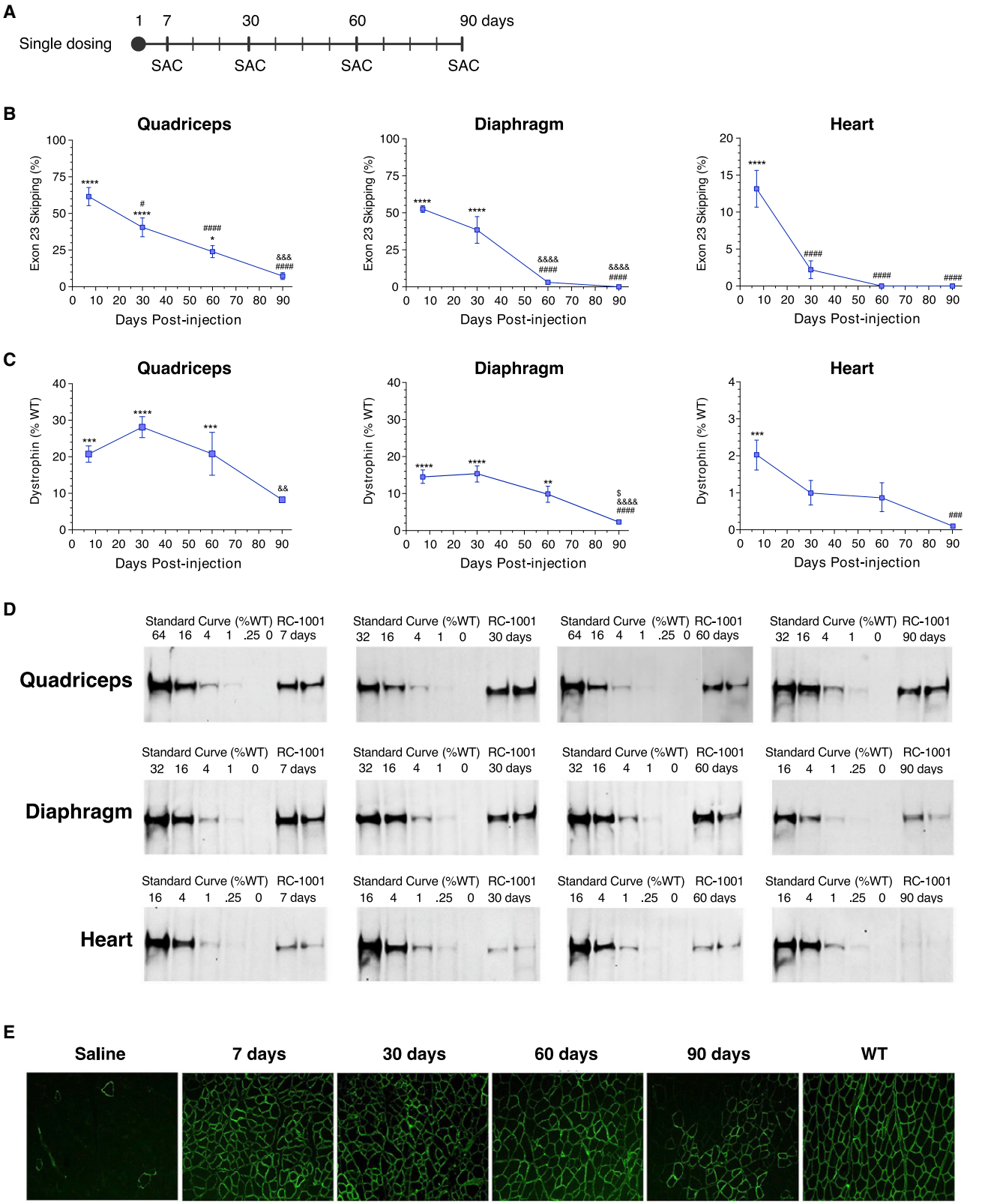

(legend on next page)

levels (day 91; 8.5%, 1.1%, and 0%, respectively; all $p < 0.005$ versus RC-1001) with the monthly dosing regimen. Immunofluorescent staining for dystrophin protein in *mdx* mice who received multiple doses of RC-1001 demonstrated that the positive fibers reached approximately 100% in the quadriceps and that the newly produced dystrophin protein was properly localized to the sarcolemma (Figure 4E).

DISCUSSION

In this study, a proprietary cell-penetrating peptide greatly increased PMO *in vivo* potency in skeletal muscle and heart in *mdx* mice. Significant increases in exon skipping and dystrophin protein levels were observed with RC-1001 compared with its counterpart PMO. After three doses of each compound, exon skipping was increased in quadriceps (98.8% versus 53.4%), diaphragm (87.4% versus 0.5%), and heart (43.2% versus 0%); importantly, these differences corresponded to equally robust differences in dystrophin protein levels (quadriceps, 38.9% versus 8.5%; diaphragm, 50.9% versus 1.1%; heart, 8.6% versus 0%). These improvements in biological efficacy afforded by the cell-penetrating peptide suggest that it enhanced cellular uptake and provided proof of concept for its utility *in vivo*. It should be noted that due to distinct differences in study designs and methodologies,[40] outcomes cannot be directly compared across studies or between different advanced treatment modalities.

Our findings also demonstrate that a single injection of RC-1001 at a dose of 40 mg/kg produced widespread, uniform staining of dystrophin-positive fibers, with dystrophin protein levels at 14.5%–20.7% for skeletal muscle and 2.0% for heart. These data demonstrate that RC-1001 40 mg/kg was more effective than a 10-fold greater dose of PMO.

RC-1001 demonstrated durability of effect up to 60 days in skeletal muscle, as measured by dystrophin protein production. Levels were increased (versus saline) by day 7 and were sustained at day 30. The decrease in dystrophin protein between days 60 and 90 indicates that the half-life of the internally truncated dystrophin protein is approximately 2 months in skeletal muscles of *mdx* mice, which is consistent with the literature.[41,42] Dystrophin protein levels remained elevated for 2 months despite a more rapid decline in exon skipping. However, repeated monthly RC-1001 doses allowed maintenance of high exon-skipping levels up to 13 weeks. As this platform is developed for the treatment of DMD, these results using the surrogate PPMO RC-1001, in conjunction with additional pre-clinical studies of the investigational PPMO SRP-5051,[43–45] support the notion of a once every 4 weeks clinical dosing regimen.

Cardiac failure is one of the leading causes of death in patients with DMD; therefore, increased levels of dystrophin protein in the heart have the potential to provide clinical benefit. Previous pre-clinical work using the same or similar oligonucleotide sequence as our experiments, but with two different chemistries (PMO and 2′-O-methyl phosphorothioate), showed limited penetration in the heart.[15,18] With a single dose of RC-1001 40 mg/kg, we observed 13.2% exon skipping and 2.0% dystrophin protein in cardiac muscle from *mdx* mice 7 days after dosing. With repeated dosing, exon skipping and dystrophin protein increased to 43.2% and 8.6%, respectively, at 13 weeks. These results demonstrate that the peptide conjugate improves delivery of the PMO to the heart. Further studies are needed to determine whether these biological effects will lead to functional cardiac benefit in humans.

In patients with DMD, inflammation and phagocytosis occur with muscle degeneration, and eventually necrotic muscle fibers are replaced by adipose and fibrous connective tissue. We observed dose-responsive reduction in mRNA levels of *Il1b* and *Tgfb1* with RC-1001 administration, suggesting that restoration of dystrophin protein in muscle reduced inflammation and fibrosis biomarkers in *mdx* mice (data not shown).

It has been challenging to determine how much dystrophin protein is sufficient to generate functional changes. Evidence from animal studies showed that a low level of newly generated dystrophin protein could be beneficial,[30,46–48] and this concept has been corroborated by evidence in humans that low residual dystrophin protein levels are associated with milder dystrophinopathy, as demonstrated by a delay in markers of disease progression such as loss of ambulation and death, compared with a complete lack of dystrophin protein.[49] Our results using lower doses of RC-1001 were consistent with this. At the 20 mg/kg dose, dystrophin protein in skeletal muscle was approximately 10% of wild type, yet we detected improved performance on rotarod and grip strength functional tests. At higher doses, performance was comparable to wild-type mice.

In summary, a proprietary cell-penetrating peptide enhanced the delivery of PPMO *in vivo* compared with its counterpart PMO, as demonstrated by increased exon skipping and dystrophin protein production in skeletal muscles and heart. These molecular effects were associated with functional recovery and were enhanced with

Figure 3. Durability of exon skipping and dystrophin protein production in the quadriceps, diaphragm, and heart muscle of *mdx* mice over 90 days following a single dose of RC-1001 40 mg/kg

(A) Timeline for single dose and tissue examination. (B) RT-PCR analysis of exon 23 skipping. Mean ± SEM, n = 6–8. (C) Western blot analysis of dystrophin protein production. Mean ± SEM, n = 6. (D and E) Representative western blot images (D) and immunofluorescent staining (E) with tissue sections from quadriceps showing dystrophin protein at the sarcolemma. One-way ANOVA with Tukey's multiple comparisons test was performed for exon skipping and dystrophin protein expression line graphs. *$p < 0.05$, **$p < 0.005$, ***$p < 0.0005$, and **** $p < 0.0001$ versus saline. #$p < 0.05$, ##$p < 0.005$, ###$p < 0.0005$, and ####$p < 0.0001$ versus day 7. &&$p < 0.005$, &&&$p < 0.0005$, and &&&&$p < 0.0001$ versus day 30. $ denotes 0.005 versus day 60. ANOVA, analysis of variance; RT-PCR, reverse transcription polymerase chain reaction; SEM, standard error of mean; WT, wild type.

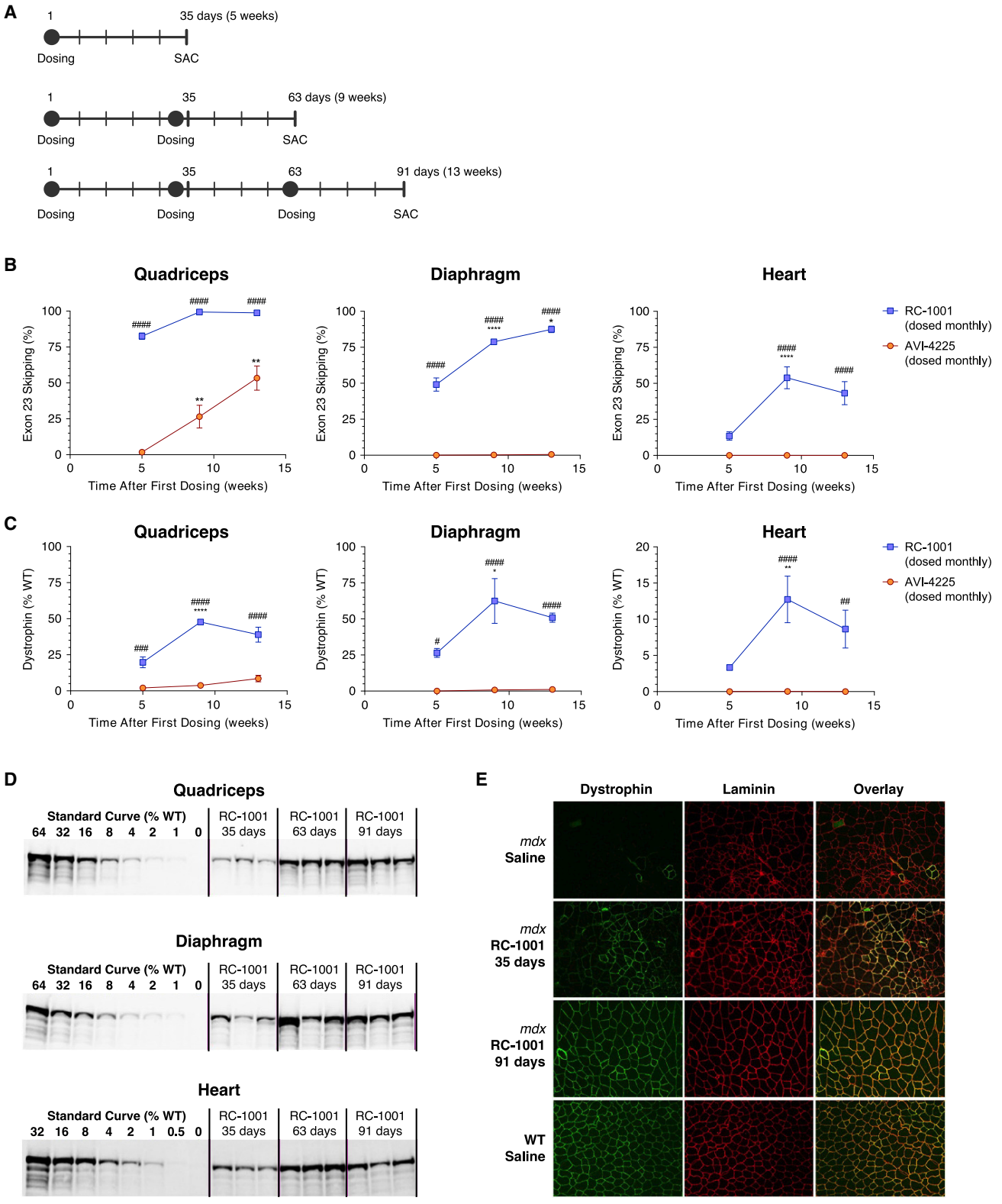

(legend on next page)

repeated monthly dosing. Although these findings were in a mouse model using a surrogate PPMO, they strongly support further development of PPMO therapies clinically. It will be important to determine PPMO potency in humans and explore a dosing regimen (once every 4 weeks) that is less frequent than the once-weekly dosing used clinically for PMO therapies. A phase 2 clinical trial evaluating the safety, tolerability, and pharmacokinetics of an exon 51-skipping PPMO, SRP-5051, containing the same cell-penetrating peptide as in the present study, is currently underway (ClinicalTrials.gov: NCT04004065).

MATERIALS AND METHODS

Animals

Single and repeated dosing of PPMO

Male *mdx* mice (C57BL/10ScSn-*DMD*^{mdx}/J, stock #001801; The Jackson Laboratory, Bar Harbor, ME, USA) and wild-type mice (C57BL/10ScSnJ, stock #000476; The Jackson Laboratory) were housed at the Sarepta Therapeutics, Inc. animal facility, where they had access to food (Labdiet 5P76; ScottPharma Solutions, Marlborough, MA, USA) and water *ad libitum*. All procedures were conducted under the guidance of an Institutional Animal Care and Use Committee.

PPMO treatment

AVI-4225 and RC-1001, with 5′-GGCCAAACCTCGGCTTACCT GAAAT-3′ PMO sequence, were manufactured at Sarepta Therapeutics, Inc. (Cambridge, MA, USA). A proprietary cell-penetrating peptide[39] was conjugated to AVI-4225 to form the RC-1001 PPMO utilized in the study.

In the PPMO dose response and functional tests study, *mdx* mice aged 7 weeks received a single tail-vein injection of RC-1001 10, 20, 40, or 80 mg/kg (n = 10 per group) and were sacrificed at 30 days post injection. Training and baseline data recording were conducted before treatment (see functional tests below). Grip strength was tested at 1 and 3 weeks after each injection. The rotarod test was conducted at 2 and 4 weeks post injection. Ten mice were tested for each dose group.

In the single-dose duration of action study, *mdx* mice aged 6 weeks received a single tail-vein injection with RC-1001 40 mg/kg (n = 24). Additional groups of *mdx* and wild-type mice (n = 8 per group) received a tail-vein injection with 200 μL saline and served as vehicle controls. The RC-1001-treated mice (n = 6 per time point) and saline-treated mice (n = 2 per time point) were sacrificed at 7, 30, 60, and 90 days post injection by carbon dioxide inhalation/anesthesia, followed by exsanguination.

In the repeated-dose study, *mdx* mice aged 6 weeks received an initial tail-vein injection with AVI-4225 or RC-1001 at 40 mg/kg (n = 18 per compound). At 11 weeks of age, 12 of these mice received a second injection of AVI-4225 or RC-1001 40 mg/kg, and 6 were sacrificed without receiving an additional injection. At 15 weeks of age, 6 mice received a third injection with AVI-4225 or RC-1001 40 mg/kg, and 6 mice were sacrificed without receiving a third injection. At 19 weeks of age, the remaining 6 animals were sacrificed. Saline-treated mice (n = 2 per time point) were also included in this study.

For the single- and repeated-dose studies, at the time of sacrifice, the diaphragm, heart, quadriceps, and biceps were harvested from each mouse and frozen for analysis of exon 23 skipping using reverse transcription polymerase chain reaction (RT-PCR), dystrophin protein expression using western blot, and dystrophin-positive fibers using immunohistochemistry.

Protein extraction and western blot analysis

For protein extraction, 7 mL homogenization buffer (4 M urea, 125 mM Tris, 4% sodium dodecyl sulfate) with one protease inhibitor cocktail tablet (Roche Applied Science, Mannheim, Germany) was added to tissue samples in a ratio from 1:10 to 1:15 (1 mg tissue:10–15 μL buffer). Tissue samples were disrupted using a cordless pellet pestle (Kimble Chase, Rockwood, TN, USA) until a fine foam was produced, indicating complete homogenization. Whole lysates were centrifuged at 15,000 × *g* for 5 min, and protein concentrations were quantified using Pierce BCA (Thermo Fisher Scientific, Waltham, MA, USA) or *RC DC* (Bio-Rad Laboratories, Hercules, CA, USA) protein assay kits, per the manufacturer's instructions.

For western blot analysis, 50 μg protein from each lysate or 15 μL HiMark pre-stained high-molecular-weight marker (Thermo Fisher Scientific) was loaded onto individual wells of 3%–8% polyacrylamide Tris-acetate gels (Thermo Fisher Scientific; Bio-Rad Laboratories). Dilutions of antibodies were prepared as follows: anti-dystrophin NCL-DYS1, 1:20 (Leica Biosystems, Buffalo Grove, IL, USA);

Figure 4. Repeated monthly dosing of PPMO and PMO in *mdx* mice

(A) Repeated 40 mg/kg monthly dosing regimen. (B) RT-PCR analysis of exon 23 skipping at 5 weeks after 1 dose, at 9 weeks (2 monthly doses), and at 13 weeks (3 monthly doses). Mean ± SEM, n = 6. Two-way ANOVA showed that time point, compound, and interaction of the two were significantly different for all three structures examined ($p < 0.005$). (C) Western blot analysis of dystrophin protein level at 5, 9, and 13 weeks after the first injection. Mean ± SEM, n = 6. Two-way ANOVA showed that time point, compound, and interaction of the two were significantly different for all three structures examined ($p < 0.005$). (D) Representative western blot images for dystrophin protein level in RC-1001-treated animals. (E) Immunofluorescent staining for dystrophin protein and laminin in quadriceps; first row shows *mdx* mice treated with saline; second row shows *mdx* mice at 90 days following a single-dose RC-1001 injection; third row shows *mdx* mice at 91 days following three monthly doses of RC-1001; and fourth row shows wild-type mice treated with saline (images, 20×). For exon skipping and dystrophin line graphs, Sidak multiple comparison test was performed to understand the differences between different time points or compounds. *$p < 0.05$, **$p < 0.005$, and ****$p < 0.0001$ versus the previous time point. ##$p < 0.005$, ###$p < 0.0005$, and ####$p < 0.0001$ versus AVI-4225. ANOVA, analysis of variance; RT-PCR, reverse transcription polymerase chain reaction; SAC, sacrifice; SEM, standard error of mean; WT, wild type.

anti-dystrophin ab15277, 1:500 (Abcam, Cambridge, MA, USA); anti-alpha actinin (sarcomeric), 1:100,000 (Sigma-Aldrich, Darmstadt, Germany); anti-sarcomeric alpha actinin ab68168, 1:10,000 (Abcam); horseradish peroxidase (HRP)-conjugated goat anti-rabbit immunoglobulin G (IgG), 1:10,000 (Bio-Rad Laboratories); HRP-conjugated goat anti-mouse IgG, 1:10,000 (Bio-Rad Laboratories); and HRP-conjugated sheep anti-mouse IgG, 1:40,000 (GE Healthcare Life Sciences, Pittsburgh, PA, USA). Images were captured and band intensities were analyzed using Chemidoc Imaging System and Image Lab software v.5.2, respectively (Bio-Rad Laboratories).

For dystrophin quantification, pooled protein lysates from wild-type mice were used as positive controls, and lysates from *mdx* mice were used as negative controls. To accurately quantify dystrophin protein levels, a standard curve with an appropriate range was applied to each gel. The serial diluted points of the standard curve were obtained by mixing the same concentration of the wild-type and DMD protein lysates. Dystrophin protein levels were analyzed using the standard curve and interpreted as the percentage of wild-type dystrophin protein expression levels.

RNA extraction and RT-PCR

Tissue samples were homogenized using a MagNA Lyser with beads at 5,000 RPM for 25 s per cycle until completely lysed. Total RNA was isolated from cooled lysates using an Illustra RNAspin 96 RNA isolation kit (GE Healthcare Life Sciences) with 96-well plates per the manufacturer's instructions. After eluting with 50 μL RNase-free water, the total RNA concentration was measured using a NanoDrop 2000 spectrophotometer (Thermo Fisher Scientific).

cDNA was generated using the SuperScript III One-Step RT-PCR System with Platinum *Taq* DNA polymerase (Invitrogen) and the following primers: mouse dystrophin exon 23 forward and reverse primers (5′-CACATCTTTGATGGTGTGAGG-3′ and 5′-CAACTT CAGCCATCCATTTCTG-3′, respectively). The RT-PCR reaction was processed at 55°C for 30 min, inactivation was processed at 94°C for 2 min, and 45 cycles were conducted for denaturing (94°C, 45 s), annealing (59°C, 45 s), extension (68°C, 1 min), and final extension (68°C, 10 min). Exon-skipping levels were analyzed using Caliper (PerkinElmer GX, Hopkinton, MA, USA) per the manufacturer's recommendations. In *mdx* mice, the PCR products included the full-length dystrophin transcript (445 base pairs [bp]) and the exon 23-skipped mRNA (232 bp).

Immunofluorescent staining

Muscles excised from wild-type or *mdx* mice were covered in OCT and laid flat on a labeled disposable freezing mold. Molds containing muscles were frozen in the chilled 2-methylbutane in a steel beaker using liquid nitrogen for 1 min and stored at −80°C. Serial tissue sections (10 μm) were rehydrated in phosphate-buffered saline (PBS) and incubated in Mouse On Mouse blocking solution (Vector Laboratories, Burlingame, CA, USA) at room temperature for 1 h. Sections were then incubated at 4°C overnight with rabbit anti-dystrophin antibody (Abcam, cat# ab15277) and rat anti-laminin alpha-2 (Sigma-Aldrich, cat#L0663) at 1:250 dilution in 1% BSA/0.3% Triton in PBS. After three washes in PBST for 10 min each, tissue sections were incubated in 1:250 dilution of Alexa Fluor 488 goat anti-rabbit (Thermo Fisher Scientific, cat#A11034) and Alexa Fluor 594 goat anti-rat (Thermo Fisher Scientific, cat#MA1-80017) at room temperature for 1–2 h. Sections were thoroughly washed after each incubation. Slides were mounted using Fluoro-Gel with DAPI (Electron Microscopy Sciences, Hatfield, PA, USA).

Functional tests

An accelerating rotarod test was performed to measure motor coordination and performance. In brief, the mice were placed on a rotarod (Ugo Basile SRL, Varese, Italy) that accelerated from 10 to 40 RPM for 5 min. Latency to fall was recorded over three trials using a 3 day protocol. On day 1, mice were acclimated to the rotarod over 2 min at 10 RPM. Each time the mouse fell, it was replaced on the rod for the full 2 min. On day 2, the mice were acclimated to the rotarod for an acceleration from 10 to 40 RPM over 30 s for 5 min. On day 3, the same protocol from day 2 was applied, but only latency to fall was recorded. A total of three trials were recorded, with 1 h of rest between each trial. Due to their training during the acclimation and conditioning period, mice never intentionally jumped from the rotarod. Rare instances of mice gripping onto the rod without being able to return to walking on the rod after three full rotations indicated impaired muscle coordination of the mice and were recorded as falls.

A grip strength test was conducted to assess maximal peak force (*g*) in *mdx* mice by following Treat-NMD standard operating procedure for the use of grip strength meter of *mdx* mice.[50] Specifically, the test was performed by a single operator at the same time of day/week. The maximum force measurement was obtained by the operator drawing the mouse along a straight line over a grid leading away from an attached sensor (Columbus Instruments, Columbus, OH, USA) when the mouse was released at the end of the grid. A mean measurement was calculated from five consecutive measurements taken at baseline and on each day of testing, which was performed weekly.

Statistics

The effect of RC-1001 treatment on levels of exon skipping, dystrophin protein and functional measures was analyzed by one-way analysis of variance (ANOVA) tests. Tukey's multiple comparison tests were used to probe differences between groups. Two-way ANOVA tests were used to analyze the effects of RC-1001 and AVI-4225 on exon skipping and dystrophin protein levels over time. Sidak multiple comparison tests were used to understand the differences between different time points or compounds. All data and statistical analyses were recorded and analyzed using GraphPad Prism 8.1.

DATA AVAILABILITY STATEMENT

Qualified researchers may request access to the data that support the findings of this study from Sarepta Therapeutics, Inc. by contacting medinfo@sarepta.com.

SUPPLEMENTAL INFORMATION

Supplemental information can be found online at https://doi.org/10.1016/j.omtn.2022.08.019.

ACKNOWLEDGMENTS

Writing support was provided by Valerie P. Zediak, PhD, of Eloquent Scientific Solutions, and this work was funded by Sarepta Therapeutics, Inc.

AUTHOR CONTRIBUTIONS

J.A.W., L.G., M.Y., C.M.T., N.L.E., M.A.P., and L.C.L.W. collaborated to perform data acquisition and analysis. L.G., M.A.P., and L.C.L.W. drafted the manuscript. All authors reviewed and edited the manuscript.

DECLARATION OF INTERESTS

This study was sponsored by Sarepta Therapeutics, Inc. B.M.W., L.C.L.W., C.M.T., G.J.H., J.A.W., L.G., M.A.P., M.Y., and N.L.E. were employees of Sarepta Therapeutics, Inc., at the time of this research. B.M.W. is currently affiliated with Dyne Therapeutics, Inc. (Waltham, MA, USA); C.M.T. is currently at Avrobio. Inc. (Cambridge, MA, USA); J.A.W. is currently at Agios Pharmaceuticals Inc. (Cambridge, MA, USA); L.G. is currently at Skyhawk Therapeutics, Inc. (Waltham, MA, USA); M.A.P. is currently at Disarm Therapeutics, Inc. (Cambridge, MA, USA); M.Y. is currently at Dyne Therapeutics, Inc. (Waltham, MA, USA); and N.L.E. is currently at Entrada Therapeutics, Inc. (Boston, MA, USA).

REFERENCES

1. Allen, D.G., Whitehead, N.P., and Froehner, S.C. (2016). Absence of dystrophin disrupts skeletal muscle signaling: roles of Ca2+, reactive oxygen species, and nitric oxide in the development of muscular dystrophy. Physiol. Rev. *96*, 253–305.
2. Bushby, K., Finkel, R., Birnkrant, D.J., Case, L.E., Clemens, P.R., Cripe, L., Kaul, A., Kinnett, K., McDonald, C., Pandya, S., et al. (2010). Diagnosis and management of Duchenne muscular dystrophy, part 1: diagnosis, and pharmacological and psychosocial management. Lancet Neurol. *9*, 77–93.
3. Kole, R., and Krieg, A.M. (2015). Exon skipping therapy for Duchenne muscular dystrophy. Adv. Drug Deliv. Rev. *87*, 104–107.
4. Mah, J.K. (2016). Current and emerging treatment strategies for Duchenne muscular dystrophy. Neuropsychiatr. Dis. Treat. *12*, 1795–1807.
5. Muntoni, F., Torelli, S., and Ferlini, A. (2003). Dystrophin and mutations: one gene, several proteins, multiple phenotypes. Lancet Neurol. *2*, 731–740.
6. Kobayashi, Y.M., and Campbell, K.P. (2012). Skeletal muscle dystrophin-glycoprotein complex and muscular dystrophy. In Muscle: Fundamental Biology and Mechanisms of Disease, *2*, J.A. Hill and O. E.N, eds. (Academic Press), pp. 935–942.
7. Kole, R., Williams, T., and Cohen, L. (2004). RNA modulation, repair and remodeling by splice switching oligonucleotides. Acta Biochim. Pol. *51*, 373–378.
8. Popplewell, L.J., Trollet, C., Dickson, G., and Graham, I.R. (2009). Design of phosphorodiamidate morpholino oligomers (PMOs) for the induction of exon skipping of the human DMD gene. Mol. Ther. *17*, 554–561.
9. Wilton, S.D., Fall, A.M., Harding, P.L., McClorey, G., Coleman, C., and Fletcher, S. (2007). Antisense oligonucleotide-induced exon skipping across the human dystrophin gene transcript. Mol. Ther. *15*, 1288–1296.
10. Wilton, S.D., and Fletcher, S. (2011). RNA splicing manipulation: strategies to modify gene expression for a variety of therapeutic outcomes. Curr. Gene Ther. *11*, 259–275.
11. Wilton, S.D., Lloyd, F., Carville, K., Fletcher, S., Honeyman, K., Agrawal, S., and Kole, R. (1999). Specific removal of the nonsense mutation from the mdx dystrophin mRNA using antisense oligonucleotides. Neuromuscul. Disord. *9*, 330–338.
12. Monaco, A.P., Bertelson, C.J., Liechti-Gallati, S., Moser, H., and Kunkel, L.M. (1988). An explanation for the phenotypic differences between patients bearing partial deletions of the DMD locus. Genomics *2*, 90–95.
13. Lebedeva, I., and Stein, C.A. (2001). Antisense oligonucleotides: promise and reality. Annu. Rev. Pharmacol. Toxicol. *41*, 403–419.
14. Miyatake, S., Mizobe, Y., Takizawa, H., Hara, Y., Yokota, T., Takeda, S., and Aoki, Y. (2018). Exon skipping therapy using phosphorodiamidate morpholino oligomers in the mdx52 mouse model of Duchenne muscular dystrophy. Methods Mol. Biol. *1687*, 123–141.
15. Wu, B., Lu, P., Benrashid, E., Malik, S., Ashar, J., Doran, T.J., and Lu, Q.L. (2010). Dose-dependent restoration of dystrophin expression in cardiac muscle of dystrophic mice by systemically delivered morpholino. Gene Ther. *17*, 132–140.
16. Yokota, T., Lu, Q.L., Partridge, T., Kobayashi, M., Nakamura, A., Takeda, S., and Hoffman, E. (2009). Efficacy of systemic morpholino exon-skipping in Duchenne dystrophy dogs. Ann. Neurol. *65*, 667–676.
17. Yin, H., Lu, Q., and Wood, M. (2008). Effective exon skipping and restoration of dystrophin expression by peptide nucleic acid antisense oligonucleotides in mdx mice. Mol. Ther. *16*, 38–45.
18. Lu, Q.L., Rabinowitz, A., Chen, Y.C., Yokota, T., Yin, H., Alter, J., Jadoon, A., Bou-Gharios, G., and Partridge, T. (2005). Systemic delivery of antisense oligoribonucleotide restores dystrophin expression in body-wide skeletal muscles. Proc. Natl. Acad. Sci. USA *102*, 198–203.
19. Exondys 51 (eteplirsen) injection, for intravenous use [Prescribing Information]. 2020. Cambridge, MA: Sarepta Therapeutics, Inc.
20. Vyondys 53 (golodirsen) injection, for intravenous use [Prescribing Information]. 2020. Cambridge, MA: Sarepta Therapeutics, Inc.
21. Viltepso (viltolarsen) injection, for intravenous use [Prescribing Information]. 2020. Paramus, NJ: NS Pharma, Inc.
22. Amondys 45 (casimersen) injection, for intravenous use [Prescribing Information]. 2021. Cambridge, MA: Sarepta Therapeutics, Inc.
23. Kinane, T.B., Mayer, O.H., Duda, P.W., Lowes, L.P., Moody, S.L., and Mendell, J.R. (2018). Long-term pulmonary function in Duchenne muscular dystrophy: comparison of eteplirsen-treated patients to natural history. J. Neuromuscul. Dis. *5*, 47–58.
24. McDonald, C.M., Shieh, P.B., Abdel-Hamid, H.Z., Connolly, A.M., Ciafaloni, E., Wagner, K.R., Goemans, N., Mercuri, E., Khan, N., Koenig, E., et al. (2021). Open-label evaluation of eteplirsen in patients with Duchenne muscular dystrophy amenable to exon 51 skipping: PROMOVI trial. J. Neuromuscul. Dis. *8*, 989–1001.
25. Mendell, J.R., Goemans, N., Lowes, L.P., Alfano, L.N., Berry, K., Shao, J., Kaye, E.M., Mercuri, E.; Eteplirsen Study Group and Telethon Foundation DMD Italian Network, and Telethon Foundation, D.M.D.I.N. (2016). Longitudinal effect of eteplirsen versus historical control on ambulation in Duchenne muscular dystrophy. Ann. Neurol. *79*, 257–271.
26. Mendell, J.R., Khan, N., Sha, N., Eliopoulos, H., McDonald, C.M., Goemans, N., Mercuri, E., Lowes, L.P., and Alfano, L.N.; Eteplirsen Study Group (2021). Comparison of long-term ambulatory function in patients with Duchenne muscular dystrophy treated with eteplirsen and matched natural history controls. J. Neuromuscul. Dis. *8*, 469–479.
27. Servais, L., Mercuri, E., Straub, V., Guglieri, M., Seferian, A.M., Scoto, M., Leone, D., Koenig, E., Khan, N., Dugar, A., et al. (2021). Long-term safety and efficacy data of golodirsen in ambulatory patients with Duchenne muscular dystrophy amenable to exon 53 skipping: a first-in-human, multicenter, two-part, open-label Phase 1/2 trial. Nucleic Acid Ther. *32*, 29–39.
28. Hammond, S.M., Aartsma-Rus, A., Alves, S., Borgos, S.E., Buijsen, R.A.M., Collin, R.W.J., Covello, G., Denti, M.A., Desviat, L.R., Echevarría, L., et al. (2021). Delivery of oligonucleotide-based therapeutics: challenges and opportunities. EMBO Mol. Med. *13*, e13243.
29. Malerba, A., Sharp, P.S., Graham, I.R., Arechavala-Gomeza, V., Foster, K., Muntoni, F., Wells, D.J., and Dickson, G. (2011). Chronic systemic therapy with low-dose

morpholino oligomers ameliorates the pathology and normalizes locomotor behavior in mdx mice. Mol. Ther. *19*, 345–354.

30. Wu, B., Xiao, B., Cloer, C., Shaban, M., Sali, A., Lu, P., Li, J., Nagaraju, K., Xiao, X., and Lu, Q.L. (2011). One-year treatment of morpholino antisense oligomer improves skeletal and cardiac muscle functions in dystrophic mdx mice. Mol. Ther. *19*, 576–583.
31. Schneider, A.F.E., and Aartsma-Rus, A. (2021). Developments in reading frame restoring therapy approaches for Duchenne muscular dystrophy. Expert Opin. Biol. Ther. *21*, 343–359.
32. Echevarría, L., Aupy, P., and Goyenvalle, A. (2018). Exon-skipping advances for Duchenne muscular dystrophy. Hum. Mol. Genet. *27*, R163–R172.
33. Abes, S., Moulton, H.M., Clair, P., Prevot, P., Youngblood, D.S., Wu, R.P., Iversen, P.L., and Lebleu, B. (2006). Vectorization of morpholino oligomers by the (R-Ahx-R)4 peptide allows efficient splicing correction in the absence of endosomolytic agents. J. Control. Release *116*, 304–313.
34. Amantana, A., Moulton, H.M., Cate, M.L., Reddy, M.T., Whitehead, T., Hassinger, J.N., Youngblood, D.S., and Iversen, P.L. (2007). Pharmacokinetics, biodistribution, stability and toxicity of a cell-penetrating peptide-morpholino oligomer conjugate. Bioconjug. Chem. *18*, 1325–1331.
35. Betts, C., Saleh, A.F., Arzumanov, A.A., Hammond, S.M., Godfrey, C., Coursindel, T., Gait, M.J., and Wood, M.J. (2012). Pip6-PMO, a new generation of peptide-oligonucleotide conjugates with improved cardiac exon skipping activity for DMD treatment. Mol. Ther. Nucleic Acids *1*, e38.
36. Fletcher, S., Honeyman, K., Fall, A.M., Harding, P.L., Johnsen, R.D., Steinhaus, J.P., Moulton, H.M., Iversen, P.L., and Wilton, S.D. (2007). Morpholino oligomer-mediated exon skipping averts the onset of dystrophic pathology in the mdx mouse. Mol. Ther. *15*, 1587–1592.
37. Jearawiriyapaisarn, N., Moulton, H.M., Buckley, B., Roberts, J., Sazani, P., Fucharoen, S., Iversen, P.L., and Kole, R. (2008). Sustained dystrophin expression induced by peptide-conjugated morpholino oligomers in the muscles of mdx mice. Mol. Ther. *16*, 1624–1629.
38. Yin, H., Moulton, H.M., Seow, Y., Boyd, C., Boutilier, J., Iverson, P., and Wood, M.J.A. (2008). Cell-penetrating peptide-conjugated antisense oligonucleotides restore systemic muscle and cardiac dystrophin expression and function. Hum. Mol. Genet. *17*, 3909–3918.
39. Hanson, G.J. (2015). Peptide Oligonucleotide Conjugates. US patent 9, 161, 948. Issued October 20.
40. Schnell, F.J., Frank, D., Fletcher, S., Johnsen, R.D., and Wilton, S.D. (2019). https://www.touchneurology.com/wp-content/uploads/sites/3/2019/04/US-Neuro-15.1_p40-46.pdf, https://touchneurology.com.
41. Verhaart, I.E.C., van Vliet-van den Dool, L., Sipkens, J.A., de Kimpe, S.J., Kolfschoten, I.G.M., van Deutekom, J.C.T., Liefaard, L., Ridings, J.E., Hood, S.R., and Aartsma-Rus, A. (2014). The dynamics of compound, transcript, and protein effects after treatment with 2OMePS antisense oligonucleotides in mdx mice. Mol. Ther. Nucleic Acids *3*, e148.
42. Wu, B., Lu, P., Cloer, C., Shaban, M., Grewal, S., Milazi, S., Shah, S.N., Moulton, H.M., and Lu, Q.L. (2012). Long-term rescue of dystrophin expression and improvement in muscle pathology and function in dystrophic mdx mice by peptide-conjugated morpholino. Am. J. Pathol. *181*, 392–400.
43. Shahid, M. (2020). Presented at: Oligonucleotide Therapeutics Society (OTS) annual Meeting. September 27–30, 2020. Virtual.
44. Wu, L. (2020). Presented at: Oligonucleotide Therapeutics Society (OTS) Annual Meeting. September 27–30, 2020. Virtual.
45. Hadcock, J. (2021). Presented at: Muscular Dystrophy Association (MDA) Virtual Clinical & Scientific Conference. March 15–18, 2021. Virtual.
46. Heemskerk, H., de Winter, C., van Kuik, P., Heuvelmans, N., Sabatelli, P., Rimessi, P., Braghetta, P., van Ommen, G.J.B., de Kimpe, S., Ferlini, A., et al. (2010). Preclinical PK and PD studies on 2'-O-methyl-phosphorothioate RNA antisense oligonucleotides in the mdx mouse model. Mol. Ther. *18*, 1210–1217.
47. van Putten, M., Hulsker, M., Young, C., Nadarajah, V.D., Heemskerk, H., van der Weerd, L., 't Hoen, P.A.C., van Ommen, G.J.B., and Aartsma-Rus, A.M. (2013). Low dystrophin levels increase survival and improve muscle pathology and function in dystrophin/utrophin double-knockout mice. FASEB J *27*, 2484–2495.
48. van Putten, M., van der Pijl, E.M., Hulsker, M., Verhaart, I.E.C., Nadarajah, V.D., van der Weerd, L., and Aartsma-Rus, A. (2014). Low dystrophin levels in heart can delay heart failure in mdx mice. J. Mol. Cell. Cardiol. *69*, 17–23.
49. de Feraudy, Y., Ben Yaou, R., Wahbi, K., Stalens, C., Stantzou, A., Laugel, V., Desguerre, I., FILNEMUS Network, Servais, L., Leturcq, F., et al. (2021). Very low residual dystrophin quantity is associated with milder dystrophinopathy. Ann. Neurol. *89*, 280–292.
50. DeLuca, A. (2019). Use of grip strength meter to assess the limb strength of mdx mice. https://treat-nmd.org/wp-content/uploads/2016/08/MDX-DMD_M.2.2.001.pdf.